





## Sex-specific regulation of microglial MyD88 in HMGB1-Induced anxiety phenotype in mice

Ashleigh Rawls<sup>a</sup> , Julia Dziabis<sup>b</sup>, Dang Nguyen<sup>b</sup>, Dilara Anbarci<sup>c</sup>, Madeline Clark<sup>d</sup>, Grace Zhang<sup>b</sup>, Kafui Dzirasa<sup>d,e,f</sup>, Staci D. Bilbo<sup>b,d,\*</sup> 

<sup>a</sup> Department of Pharmacology, Duke University, Durham, NC, United States of America

<sup>b</sup> Department of Psychology and Neuroscience, Duke University, Durham, NC, United States of America

<sup>c</sup> Department of Cell Biology, Duke University, Durham, NC, United States of America

<sup>d</sup> Department of Neurobiology, Duke University, Durham, NC, United States of America

<sup>e</sup> Department of Psychiatry and Behavioral Sciences, Duke University, Durham, NC, United States of America

<sup>f</sup> Howard Hughes Medical Institute, Chevy Chase, MD, United States of America

### ABSTRACT

Stress is a significant risk factor for the development and recurrence of anxiety disorders. Stress can profoundly impact the immune system, and lead to microglial functional alterations in the medial prefrontal cortex (mPFC), a brain region involved in the pathogenesis of anxiety. High mobility group box 1 protein (HMGB1) is a potent pro-inflammatory stimulus and danger-associated molecular pattern (DAMP) released from neuronal and non-neuronal cells following stress. HMGB1 provokes pro-inflammatory responses in the brain and, when administered locally, alters behavior in the absence of other stressors. In this study, we administered dsHMGB1 into the mPFC of male and female mice for 5 days to investigate the cellular and molecular mechanisms underlying HMGB1-induced behavioral dysfunction, with a focus on cell-type specificity and potential sex differences. Here, we demonstrate that dsHMGB1 infusion into the mPFC elicited behavior changes in both sexes but only altered microglial morphology robustly in female mice. Moreover, preventing microglial changes with cell-specific ablation of the MyD88 pathway prevented anxiety-like behaviors only in females. These results support the hypothesis that microglial MyD88 signaling is a critical mediator of HMGB1-induced stress responses, particularly in adult female mice.

### 1. Introduction

Anxiety is a common cause of mental health-related disability (Amer et al., 2021; Angum et al., 2020; Anxiety disorders, 2023). Anxiety disorders describe a class of disorders in which the affected person experiences consistent and often unfocused anxiety and worry (Bandelow and Michaelis, 2015). Though generally high in prevalence in both sexes, anxiety is twice as common in women throughout their lifetime (McClean et al., 2011). Few biological mechanisms have been elucidated that explain the increased prevalence of depression or anxiety in women (Rainville and Hodes, 2019); however, we do understand that stress is a pivotal factor in the development and recurrence of anxiety disorders regardless of sex or age (McEwen and Akil, 2020; Deppermann et al., 2014; Park and Kim, 2020).

Stress instigates many alterations throughout the brain-body axis (Fonken et al., 2018a,b). Specifically, changes in the peripheral and central immune systems have been observed in patients with anxiety and comorbid depression (Costi et al., 2021; Brydges et al., 2022). Preclinical models also show immune responses to physical and

psychological stressors (Ménard et al., 2017; Kokkosis et al., 2024). Psychological stress acts as a sterile immune challenge that elicits proinflammatory responses centrally and peripherally (Hodes et al., 2014, 2015). Sterile immune responses increase the release of danger-associated molecular patterns (DAMPs), which are recognized by conserved pattern recognition receptors (PRRs) primarily on immune cells. This response has been demonstrated to be an essential mechanism by which stress elicits behavioral changes (Weber et al., 2019). High mobility group box one (HMGB1) is one such DAMP released during stress that activates multiple PRRs, including toll-like receptors (TLRs) and the receptor for advanced glycation end products (RAGE) (Kang et al., 2014; Zhang et al., 2020). Previous results demonstrate that stress is associated with increased HMGB1 release in the brain and subsequent activation of TLR2, TLR4, and RAGE signaling (Pluma-Pluma et al., 2024; Chen et al., 2023). However, the mechanisms by which HMGB1 can impact behavioral sequelae such as increasing anxiety-like behavior is not well understood in cell type-specific manner.

This is due in large part because nearly all cell types express HMGB1 or one of its putative receptors within the brain and little work has been

\* Corresponding author. Department of Psychology and Neuroscience, Duke University, Durham, NC, United States of America.

E-mail address: [staci.bilbo@duke.edu](mailto:staci.bilbo@duke.edu) (S.D. Bilbo).

done to investigate the cell type specificity of HMGB1 signaling in stress responses in the brain (Fonken et al., 2016). Microglia, the resident innate immune cells of the brain, play key roles in proinflammatory signaling (Lenz and Nelson, 2018; Nimmerjahn et al., 2005) in response to stress (Cathomas et al., 2022; Mondelli et al., 2017) and express PRRs at high levels relative to other CNS cells. Microglia can respond broadly to PRR ligand binding via multiple functional alterations, including increased lysosomal activity, cytokine release and direct interactions with neurons (Fleshner et al., 2017). Genetic deletion of *Tr2/4* in microglia yields a highly stress-resilient phenotype (Nie et al., 2018). Therefore, we hypothesized that microglia have a key role in the mechanisms by which increased HMGB1 causes immune activation in the CNS and alters behavior.

To test this hypothesis, we utilized disulfide HMGB1 (dsHMGB1) locally infused into the medial prefrontal cortex (mPFC), a highly interconnected brain region critical for regulating stress responses and emotional behaviors. The mPFC integrates inputs from limbic structures, such as the amygdala and hippocampus, and exerts top-down control over hypothalamic-pituitary-adrenal (HPA) axis activity, which is essential for modulating stress reactivity and adaptive responses (Carvalho-Netto et al., 2011; Hinwood et al., 2012; Tynan et al., 2010). Dysfunction in mPFC circuits has been implicated in the pathophysiology of stress-related disorders such as anxiety and depression (Kenwood et al., 2022; Zhang et al., 2020).

HMGB1 exists in multiple redox forms, and previous studies demonstrate that both disulfide and fully reduced HMGB1 alter behavior, unlike non-oxidized HMGB1. DsHMGB1 is an established pharmacological stressor that alters depressive-like behavior when circulated throughout the whole brain via direct infusion (Lian et al., 2017). Here, we utilize localized administration of dsHMGB1 to focus on the mPFC including surrounding areas, the infralimbic cortex and anterior cingulate cortex, aiming to dissect region-specific contributions to behavior and immune signaling in the context of stress.

We found that dsHMGB1 locally administered to the mPFC produces a robust and reproducible anxiety-like phenotype in both male and female adult mice. Additionally, we observed striking sex-specific differences in microglial morphology and transcriptional activity following dsHMGB1 infusion. Notably, in females, conditional knockout of myeloid differentiation adaptor protein 88 (*Myd88*)—a critical adaptor protein for many pattern recognition receptors (PRRs)—in microglia prevented cellular morphology changes and anxiety-like behavior induced by dsHMGB1 infusion.

## 2. Results

### 2.1. HMGB1 infusion into the mPFC increases anxiety-like behavior in males and females

HMGB1 has been previously shown to increase anhedonia-like behavior (Wang et al., 2018). However, no studies to date have utilized HMGB1 as a pharmacological stressor in female subjects, calling into question how relevant sterile inflammatory mechanisms are to the stress response in females. Here, we sought first to define the impact of sub-chronic exposure to a stress-related danger signal on behavior in male and female mice. To do so, mice were infused via cannula with dsHMGB1 once daily for 5 consecutive days. Behaviors related to anxiety, sociability, and anhedonia were assessed following HMGB1 infusion into the mPFC.

Anxiety-like behavior was assessed by measuring center exploration time in the open field test (Fig. 1B), open arm exploration and latency to explore open arms of the elevated plus maze (EPM) (Fig. 1F–I), and latency to feed in a novelty suppressed feeding assay (Fig. 1I). We found that exploration of the open arms in the EPM was significantly decreased in mice treated with dsHMGB1, main effect of treatment,  $F(1, 36) = 3.608$ ,  $p = 0.0030$ . EPM Latency was significantly increased, main effect of treatment,  $F(1, 36) = 8.136$ ,  $p = 0.0148$ . In addition, we found that

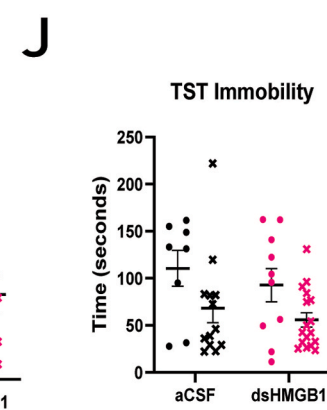
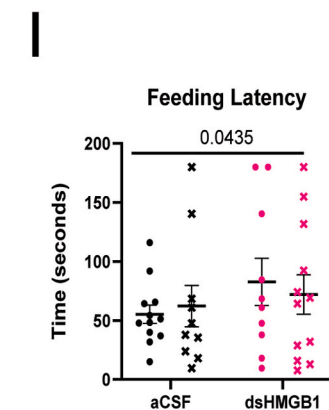
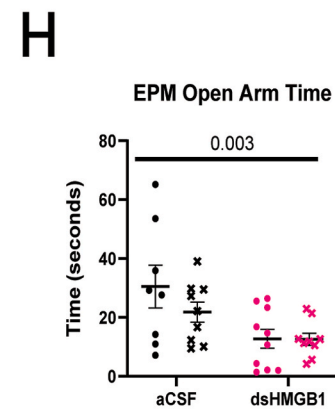
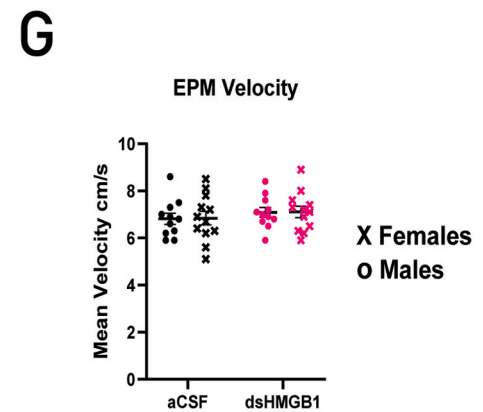
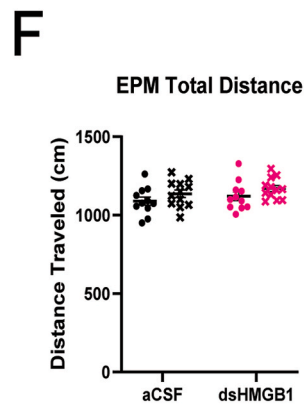
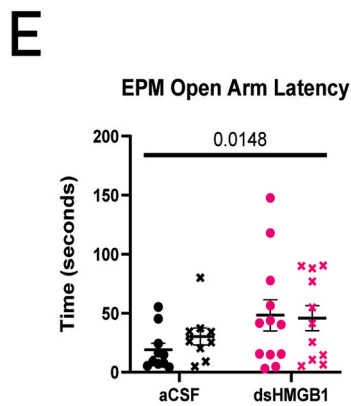
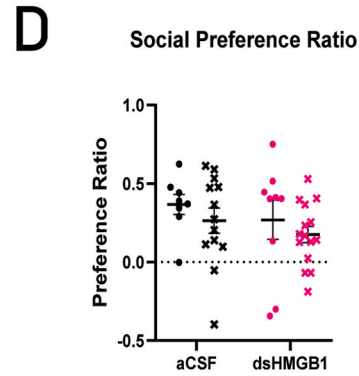
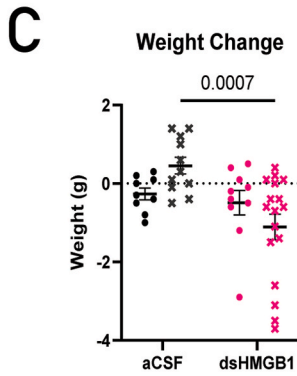
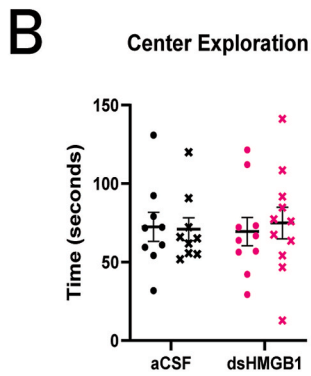
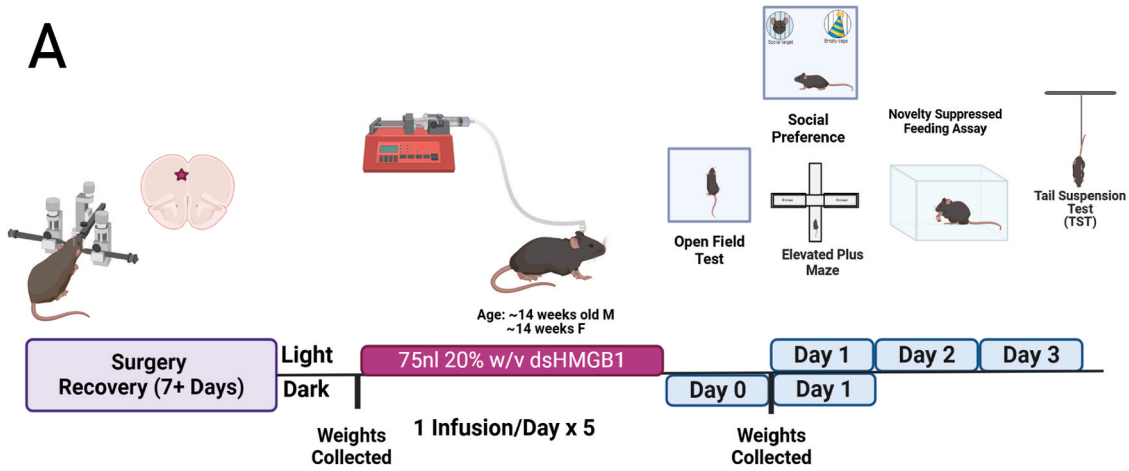
there was a significant main effect of treatment in the Home Cage Feeding latency,  $F(1,44) = 4.322$ ,  $p = 0.0435$  (Fig. 1I). No changes in social preference or behavior in the tail suspension test were found (Fig. 1C and J). The results show that dsHMGB1 infusion to the mPFC selectively alters some measures of anxiety, and this phenotype is shared between males and females. Furthermore, we found that females specifically had a significant decrease in weight following dsHMGB1 treatment, interaction effect,  $F(1,43) = 4.844$ ,  $p = 0.0053$  (Fig. 1C). We monitored estrus cycle in females on each day behavior was tested. Due to the high variability of  $n$  in each group at a given collection, we ran non-parametric statistics and compared the medians between groups in the assays with significant treatment effects. We found no significant correlation between estrus cycle and either weight loss or novelty-suppressed feeding in response to dsHMGB1 (Suppl. Figs. 1A–B). All remaining behavioral measures were insufficiently powered to assess impacts of estrus, due to most female mice falling in the same part of the cycle at the time of testing. Taken together, these results demonstrate that dsHMGB1 elicits a shared behavioral phenotype of increased anxiety-like behavior in male and female mice.

### 2.2. Microglial reactivity is stronger in females following dsHMGB1 infusion to mPFC

The mPFC is often described as a key node for stress responsiveness and emotional processing; these are key processes in the context of anxiety. Sex differences in stress-associated microglial functional changes are well documented (Bollinger et al., 2016; González Ibáñez et al., 2023). We sought to determine if microglia transcriptional and morphological changes would be a shared phenotype between males and females underlying the similar behavioral outcomes. In a smaller cohort of mice, we repeated the implantation and dosing scheme as outlined in the previous section. 16 h after the final infusion of dsHMGB1, mice completed the elevated plus maze assay and were immediately sacrificed for tissue collection. Again, an anxiety phenotype in the EPM was observed in males and females (Suppl. Fig. 2A and 2B). We triple stained Iba1, Tmem119, and CD68 to distinguish between surveillant/homeostatic, and reactive/phagocytic microglia respectively. We quantified the volume of Iba1 (Fig. 2B and F) and Tmem119 (Suppl. Fig. 2D and 2E). We utilized a nested *t*-test to compare treatment groups within sexes. There was no significant difference in Tmem119 vol alone for males or females; however, Iba1 volume differed significantly in females (1647 vs. 893.4  $\mu\text{m}^3$ ; CI 95 %, 73.79 to 1434;  $p = 0.0358$ ) (Fig. 2F). We then calculated the ratio of Tmem119 normalized to Iba1 for each reconstructed cell. We interpret this measurement as a ratio of homeostasis, as Tmem119 is often downregulated in the context of inflammation, injury, or disease progression (Spiteri et al., 2021). We observed a clear linear relationship between Iba1 volume and Tmem119 in control mice (Suppl. Fig. 2F). However, in dsHMGB1 treated mice we found this relationship was significantly altered in females but not males (Fig. 2C and G). Female mice treated with dsHMGB1 showed decreased Tmem119:Iba1 relative to controls (0.9163 vs. 1.481; CI 95 %,  $-1.048$  to  $-0.08094$ ;  $p = 0.0301$ ) (Fig. 2I). Next, we calculated phagocytic capacity by normalizing CD68 vol to Tmem119 and Iba1 merged volumes. Females but not males treated with dsHMGB1 had significantly increased lysosomal volume (5.275 vs. 1.829; CI 95 %, 0.2604 to 6.632;  $p = 0.0389$ ) (Fig. 2J). Finally, we examined changes in morphology by calculating the number of Sholl intersections using concentric distances from the radius of each cell soma. In both males and females, dsHMGB1 decreases the number of intersections and we interpret this to reflect a decrease in complexity and an increase in reactivity (Fig. 2E and I).

### 2.3. dsHMGB1 exerts sex specific changes in RAGE/MyD88 signaling

Noting the sex-specific effects of dsHMGB1 on microglial measures, we hypothesized there could also be sex-specific changes in gene expression canonically associated with a proinflammatory state. HMGB1



(caption on next page)

### Fig. 1. HMGB1 infusion to mPFC causes specific anxiety-like behavior

(A) Schematic of Experimental Workflow and Protocols (B) Center Exploration of the OFT is unchanged by HMGB1 (C) Weight Decrease Associated with dsHMGB1 Infusion is Specific to Females (D) Social Preference is not altered by HMGB1 (E) Elevated Plus Maze Open Arm Exploration (F) Elevated Plus Maze Latency to Explore Open Arms (G) Total Distance Traveled in EPM is consistent between sex/treatment groups (H) Mean Velocity in EPM is not significantly impacted by sex or treatment (I) Home cage Feeding Latency (J) TST Immobility is not significantly affected by HMGB1 Statistical analyses were performed using 2-way ANOVA to confirm primary effect of treatment and a Bonferroni post-hoc test is displayed on each graph. (\* $p < 0.05$ , \*\* $p < 0.01$ ),  $n = 8$ – $12$  mice for each group Results are expressed as the mean  $\pm$  SEM.

is a putative ligand for TLR4 and RAGE receptors (Xu et al., 2019; Pluma-Pluma et al., 2024; Sparvero et al., 2009). Canonical activation of either of these receptors requires subsequent binding of the adaptor protein MyD88 (Yao et al., 2023). We utilized a CD11b + cell specific isolation protocol where CD11b marks myeloid cells, which are solely expressed by microglia and macrophages in the intact brain. CD11b- and CD11b + cell fractions were isolated from mice 16 h after the final dose to maintain the same timeframe as behavioral and immunohistochemical experiments. All cells were isolated from the frontal cortex (Bregma 2.62 – Bregma 1.15), including tissue with primarily PFC as well as surrounding areas containing the infralimbic, cingulate, and motor cortex.

In males, no significant changes were found in *Tlr4*, *Rage*, or *Myd88* in CD11b + cells. However, we did identify a main effect of cell type,  $F(1,12) = 8.994$ ,  $p = 0.0111$  for Male TLR4 (Fig. 3A). In females we found a main effect of treatment in all measured genes. CD11b + cells showed significant increases in *Tlr4*,  $F(1,14) = 4.712$ ,  $p = 0.0476$ , Bonferroni's Post-Hoc  $p < 0.0001$  (Fig. 3E); as well as *Rage*,  $F(1,14) = 13.52$ ,  $p = 0.0025$ , Bonferroni's post-hoc  $p = 0.0003$  (Fig. 3D); and *Myd88*,  $F(1,14) = 18.25$ ,  $p = 0.0008$ . Bonferroni's post-hoc  $p < 0.0001$  (Fig. 3F).

#### 2.4. Microglial MyD88 is necessary for HMGB1-induced anxiety in females

To test the hypothesis that microglial MyD88 is necessary for anxiety-like behavioral responses to HMGB1, we utilized our previously characterized mouse line that has conditional deletion of the *Myd88* gene for CX3CR1 expressing cell types (Rivera et al., 2019; Smith et al., 2020), which includes all microglia in the CNS (Suppl. Fig 4). We first investigated the microglial specific response to dsHMGB1 administration in control and cKO mice. To do so all animals were administered dsHMGB1 for 5 days as previously described (Fig. 1A). We utilized IHC to assess reactivity changes in microglia in the mPFC as before. No significant genotype differences in dsHMGB1 response were observed in males. In contrast, we found that female cKO mice have increased TMEM119: Iba1 ratio (Fig. 4H) compared to control females (0.9138 vs. 1.407, 95 % CI 0.1199 to 0.8674,  $p = 0.0167$ ), as well as decreased lysosomal volume (Fig. 4I) (5.166 vs. 2.329, 95 % CI -4.890 to -0.7852,  $p = 0.0151$ ), indicating a rescue/prevention of dsHMGB1-induced microglial changes in females.

Both male and female control mice responded with an anxiety-like phenotype following dsHMGB1 treatment as we have seen previously. Both male and female Cre- (control) mice show a main effect of treatment in EPM Exploration,  $F(1,24) = 17.63$ ,  $p = 0.0003$  (Fig. 5B);  $F(1,20) = 0.0033$  (Fig. 5C). cKO males looked similar to control mice, demonstrating increased latency in the NSF. We report a main effect of treatment for males in the NSF,  $F(1,21) = 24.26$ ,  $p < 0.0001$  (Fig. 5D). However, female cKO mice do not demonstrate an anxiety-like phenotype in the EPM, main effect of interaction,  $F(1,20) = 8.567$ ,  $p = 0.0081$  (Fig. 4C), or in the Novelty Suppressed Feeding (NSF) assay,  $F(1,21) = 24.26$ ,  $p < 0.0001$  (Fig. 5E).

### 3. Discussion

Understanding cell-type specific mechanisms of stress response may facilitate improved treatment of disorders of which stress is a key precipitating factor, like depression and anxiety. The hypothesis that inflammation is a critical mechanism which drives behavioral changes

after stress exposure has a substantial precedent in the literature (Won and Kim, 2020; Frank et al., 2018). Previous studies demonstrate that anti-inflammatory treatments can prevent and/or reverse behavioral deficits caused by stress in preclinical models (Bassett et al., 2021). However, non-specific anti-inflammatory treatment is likely not sufficient or ideal to treat anxiety in humans (Hellmann-Regen et al., 2022). Therefore, more work is needed to unravel mechanisms of stress induced neuroinflammation to determine if therapeutics can be more precisely targeted.

HMGB1 preclinical models are emerging as a robust and reliable way to induce stress-associated behavioral effects (Huang et al., 2023). HMGB1-induced behavioral changes are reversed by antidepressants as well as the anti-inflammatory drug minocycline (Wang et al., 2019). More recent studies, including this one, demonstrate dsHMGB1's utility as a pharmacological stressor which can impact specific behavior based on site of drug delivery. Moreover, dsHMGB1 does so while enacting other physiological changes associated with stress, e.g. weight loss in females, potentially providing novel insights into the pathophysiology of anxiety disorders.

Though anxiety and depression are twice as common in women, the current body of work related to stress, anxiety, and depression has been done primarily in male subjects (Kalin, 2020; Farhane-Medina et al., 2022). Pre-clinical stress models do not utilize female subjects to a comparable degree as male subjects nor to a degree that mimics the increased prevalence of these disorders in women (Lopez and Bagot, 2021). Various models of stress are utilized throughout the field, each exerting both specific and generalizing effects (Saxena et al., 2020). A now growing body of work is revisiting these canonical mechanisms of stress response in female subjects (Yin et al., 2019) and uncovering both convergence and distinct mechanisms compared to males (Baugher et al., 2022; González Ibáñez et al., 2023; Woodburn et al., 2021). In the present study our findings echo this trend; male and female adult mice infused with dsHMGB1 in the mPFC exhibit a shared anxiety-like phenotype in the EPM and NSF assay. However, the mechanisms were distinct, as changes in microglial reactivity were not evenly observed in both sexes.

Increased microglial reactivity may be a necessary mechanism by which stress alters behavior (Lehmann et al., 2018, 2019). Very little is established in the literature concerning understanding HMGB1-induced cellular mechanisms in a cell-specific manner. We hypothesized that increased microglial reactivity via PRRs would prove to be a crucial mechanism by which HMGB1 induces behavioral changes. We examined several previously identified hallmarks of stress-associated microglial pathology. Only females demonstrated significant alterations in microglia volume, lysosomal volume, and homeostatic marker expression in C57BLJ/6 mice. Similarly, females specifically displayed significant increases in transcription of *Tlr4*, *Rage*, and *Myd88* in microglial cells isolated from the frontal cortex. The role of microglial RAGE in the context of stress was first identified in male rats (Franklin et al., 2018). Here we demonstrate that adult female mice display increased ligation of microglial *Rage*, *Tlr4* and *Myd88* following dsHMGB1 infusion. Finally, to elucidate the specificity of this MyD88-dependent PRR driven mechanism, we investigated how previously established phenotypes of behavioral changes and robust morphological changes would be affected in the cKO condition. We found that cKO females only showed prevention of behavioral changes and microglial reactivity. From this we conclude that microglial MyD88 is key for HMGB1 associated behavioral changes and we believe this may have high relevance for

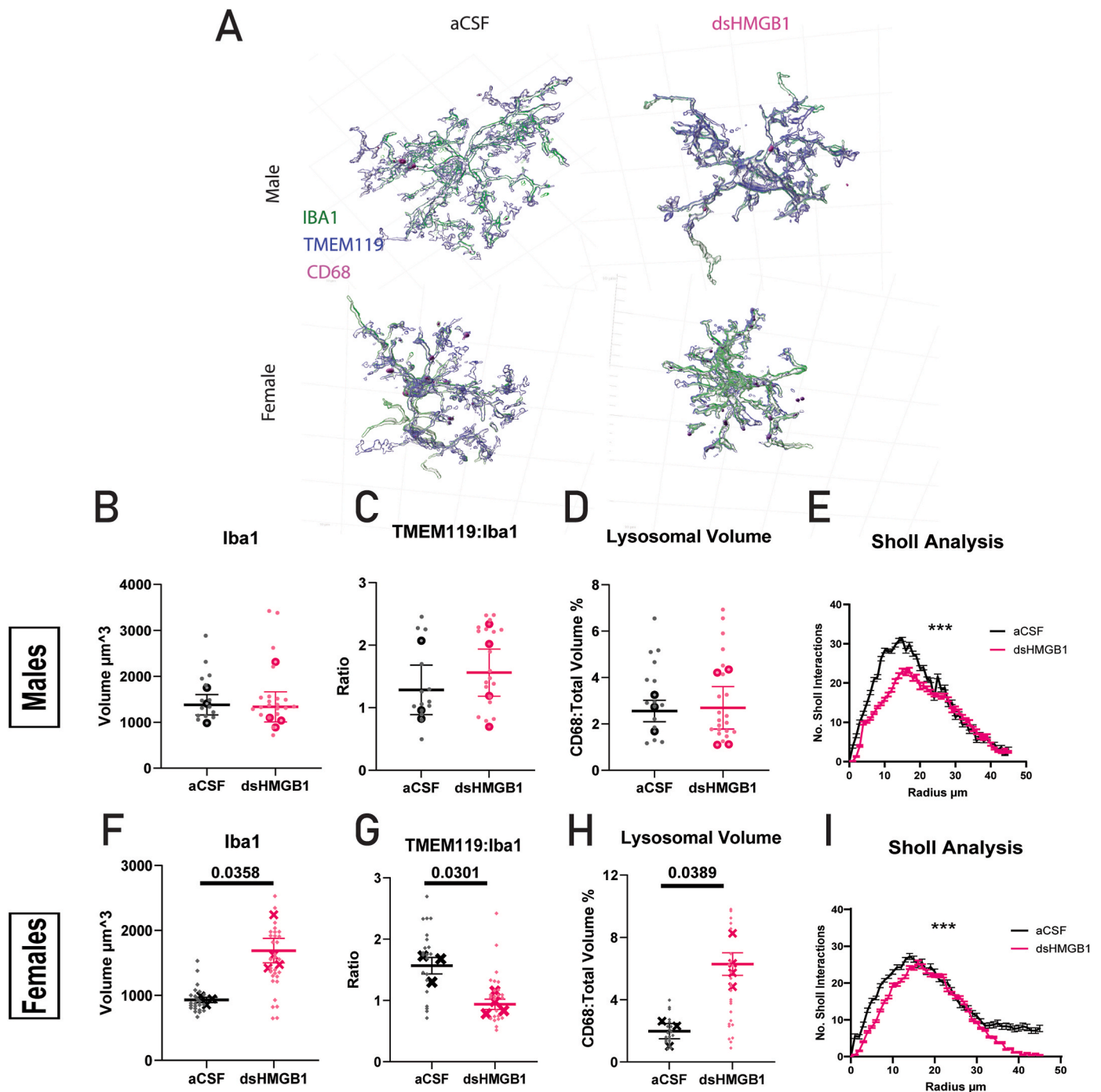


**Fig. 2.** HMGB1 infusion induces morphological changes primarily in female microglia (A) Representative Images for IHC analysis (B–E) Microglial imaging analysis for male mice (B) Iba1 Volume Quantification (C) Tmem119:Iba1 Volume Ratio (D) Lysosomal Volume was calculated by normalizing total CD68 vol to the total volume of IBA1 and Tmem119 merged. (E) Male Microglia Have Significantly Altered Morphology following HMGB1 (F–I) Microglial imaging analysis for female mice. (F) Iba1 Volume Quantification (G) Tmem119:Iba1 Volume Ratio (H) Lysosomal Volume Lysosomal volume was calculated by normalizing total CD68 vol to the total volume of IBA1 and Tmem119 merged. (I) Female Microglia Have Significantly Altered Morphology following HMGB1 Statistical analyses were performed using nested *t*-test apart from Sholl Analysis. Statistical analysis for this measure was performed by comparing the Pearson *r* values of the aCSF condition and dsHMGB1 condition (\**p* < 0.05, \*\**p* < 0.01, *n* = 3–4 mice for each group, each mouse has an *n* = 6–9 cells that were 3D reconstructed for analysis). Each larger dot represents an individual mouse, and each smaller symbol represents individual cells. Results are expressed as the mean ± SEM.

sex-specific mechanisms of stress.

We must acknowledge several limitations with our study. Firstly, we infused 75 nL of 20 % dsHMGB1 into the mPFC once daily for five consecutive days. This dose was first validated by its ability to significantly alter anxiety-like behaviors in males. We then utilized this same dosing scheme in the female experimental group. Due to all animals

being of adult age 13–20 weeks, we did not adjust dosing based on weight since direct infusion allows the bypassing of peripheral absorption routes. A previous study utilizing dsHMGB1 at a significantly higher dose and over a longer period reports a similar behavioral effect (Du et al., 2022). It is possible that some findings may be dose dependent. Specifically, the transcriptional responses in male microglia trend in

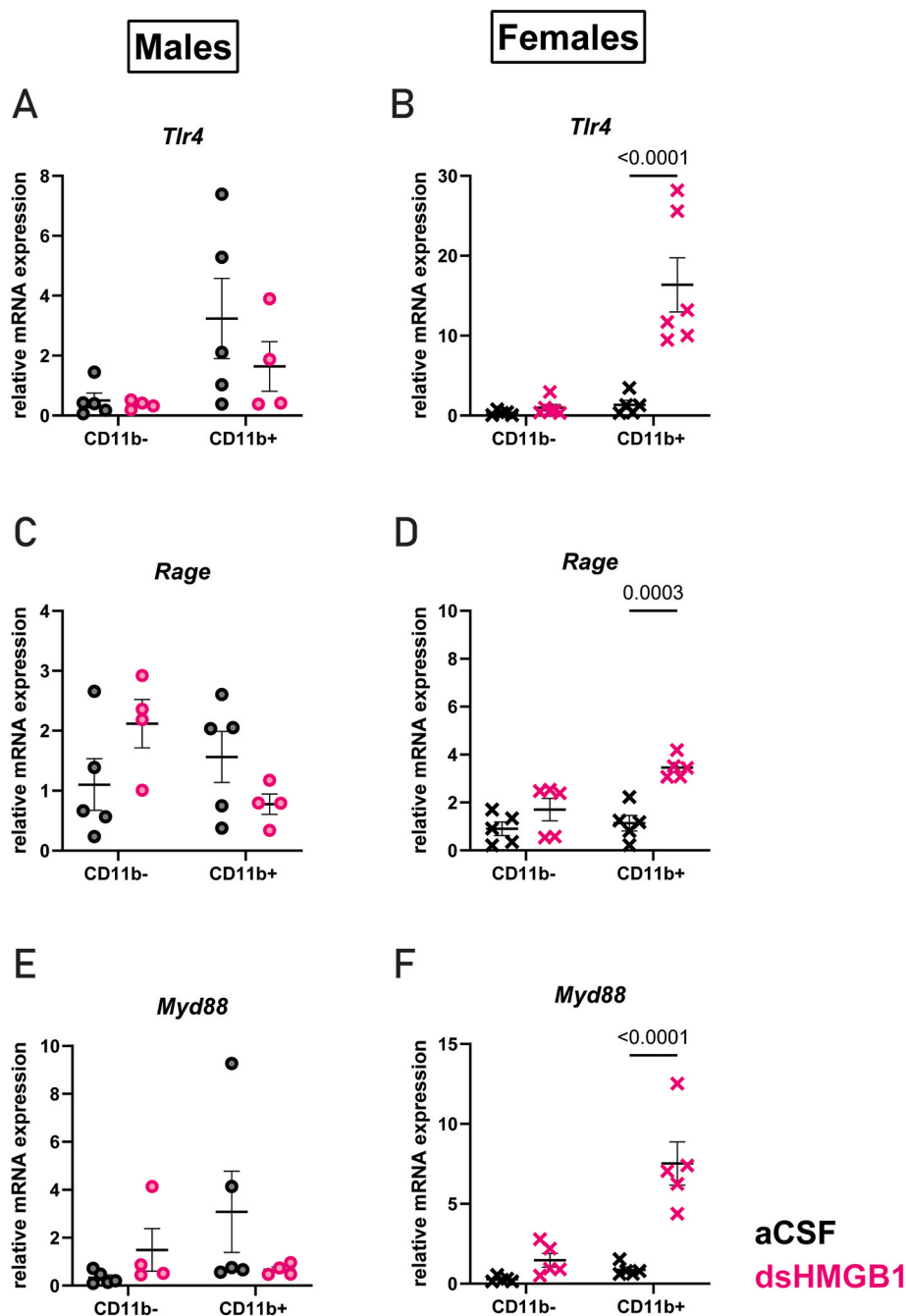


**Fig. 3.** Male and Female Microglia Display Differential Transcriptional Responses to HMGB1

16 h following the final infusion of HMGB1, mice were sacrificed, and the frontal cortex was collected for cell isolation protocol as described in methods and materials section. CD11b + cells are microglia and CD11b-cells are inclusive of neurons, astrocytes, and other glia (A) Male Expression of TLR4 (B) Female Expression of TLR4 (C) Male Expression of RAGE (D) Female Expression of RAGE (E) Male Expression of MyD88 (F) Female of Expression of MyD88. Statistical analyses were performed using 2-way ANOVA and Bonferroni post-hoc test values are displayed if adjusted  $p < 0.05$  ( $n = 4-5$  mice for each group, each). Each dot represents an individual mouse. Results are expressed as the mean  $\pm$  SEM.

opposite directions than females. This was not surprising as it has been previously demonstrated that sub-chronic stress transiently down-regulates RAGE and TLR4 in male rodent models (Franklin et al., 2018a, b). However, it highlights the importance of potentially utilizing this model in both sexes across a broader dosing range to better delineate the tunability of HMGB1 responses. In addition, it is exciting to report results from the first utilization of dsHMGB1 as a pharmacological stressor in normally cycling females. Mice typically cycle across a period of 4–5 days. Both dosing and the initial behavior battery occurred over a period of 4–5 days meaning mice were dosed and assayed at each point in their

cycle. We were under-powered to investigate potential hormonal mechanisms more thoroughly in this study, but it is a possibility that warrants future investigation.

Finally, and possibly most importantly, it would be exciting to draw broader conclusions about the role of microglial MyD88 in the physiological stress response, e.g. in response to psychological distress models. However, more work is needed to understand the role of microglial MyD88 in the stress response in such a way that generalizes across stress models.

There are several interesting future directions based on the findings

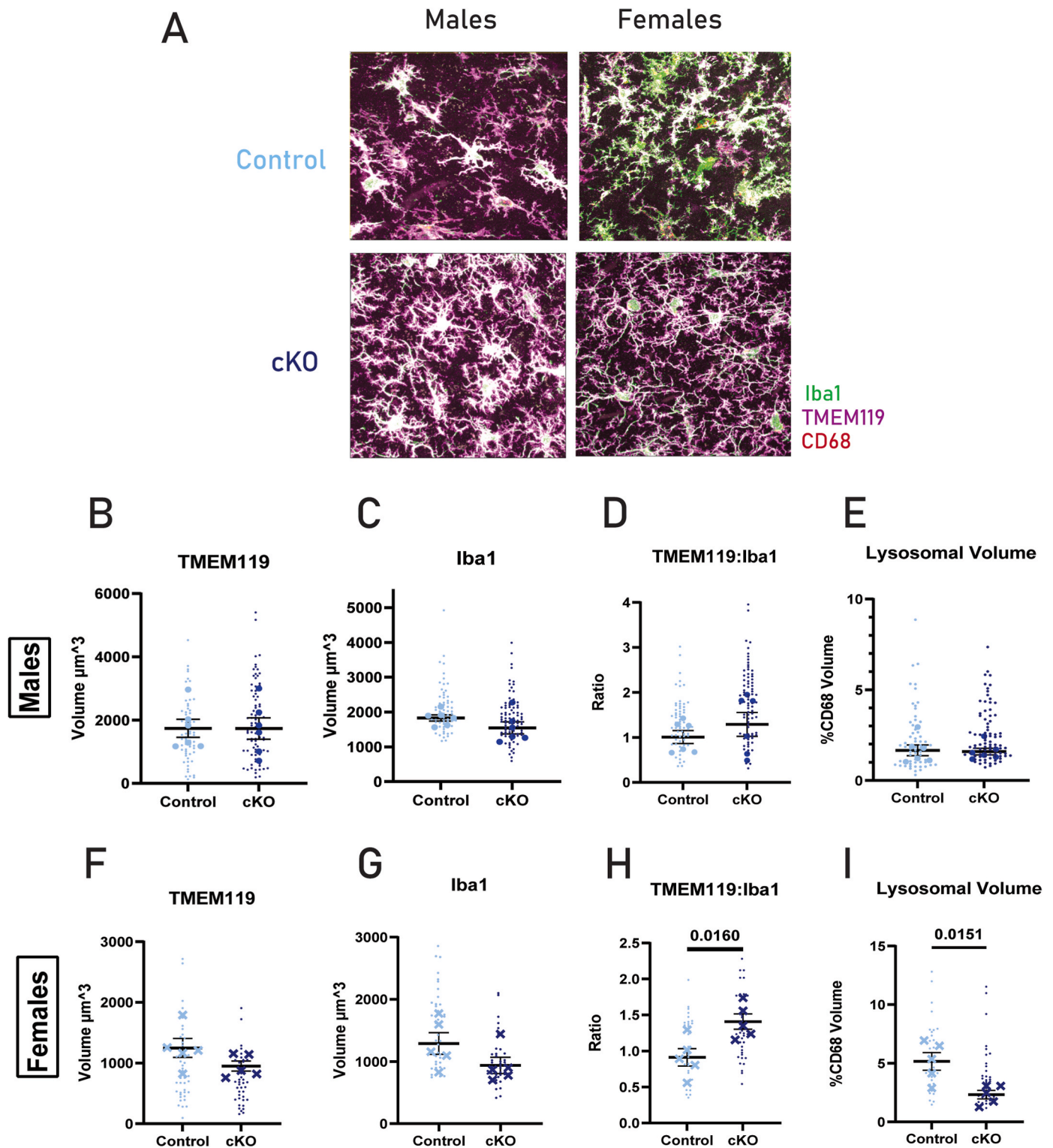


**Fig. 4.** Microglial Reactivity changes are prevented in cKO Females

(A) Representative fields of view for male and female control and cKO mice that received dsHMGB1 into the mPFC (B–E) Microglial imaging analysis for male mice (B) Tmem119 vol Quantification (C) Iba1 Volume Quantification (D) Tmem119:Iba1 Volume Ratio (E) Lysosomal Volume. (F–I) Microglial imaging analysis for female mice (F) Tmem119 vol Quantification (G) Iba1 Volume Quantification (H) Tmem119:Iba1 Volume Ratio (I) Lysosomal Volume. Statistical analyses were performed using nested *t*-test apart (\**p* < 0.05, \*\**p* < 0.01, *n* = 5–7 mice for each group, each mouse has an *n* = 8–11 cells that were 3D reconstructed for analysis). Each larger dot represents an individual mouse, and each smaller symbol represents individual cells. Results are expressed as the mean  $\pm$  SEM.

of this study. Now that we have elucidated the importance of microglial MyD88 in female HMGB1 response, understanding the time course of resolution as well as investigating how this mechanism relates to stress-induced priming would be an interesting investigational aim. In line with this, we observed an almost bivalent effect of dsHMGB1 at this dose in both males and females. As previously stated, we utilized a significantly lower dose of dsHMGB1 that we believe allowed us to potentially capture a pseudo resilient v. Susceptible phenotype. It would be interesting to follow up this observation with studies that examine how HMGB1-induced responses correlate with the response to stressors and subthreshold stressors. The male data in this study is quite interesting, though we observed behavioral changes in response to dsHMGB1 administration, the microglia reactivity changes were not as robust as in females. Further studies could investigate if another glial and/or neuronal-mediated mechanism underlie male response to HMGB1.

This study adds to a growing body of work that demonstrates that similar behavioral response following stress may be the result of distinct sex-specific mechanisms (Woodburn et al., 2021; Yao et al., 2023). We also report the first use of dsHMGB1 as a model of anxiety in female adult mice. Models of localized HMGB1 drug delivery could be utilized to further probe the effects of neuroinflammation with increased specificity. Expanding our understanding of mechanisms upstream of HMGB1 release as well as downstream signaling could continue to provide novel insights into stress pathology and other disease etiology (Xue et al., 2021; Yang et al., 2021) with potential broader implications. This work highlights the importance of utilizing both males and females in studies, when applicable, to identify sex-specific effects and/or shared phenotypes between sexes (Labonté et al., 2017).

Beyond the potential utility of HMGB1, this study highlights an important and potentially necessary role for microglia in female behavioral responses to increased extracellular alarmins. Increased extracellular alarmins are commonly associated with stress (Zhang et al., 2020); however, they are also observed in auto-immune diseases (Desai and Brinton, 2019). Microglia and macrophages have a demonstrated role in stress-associated psychiatric conditions (Shimo et al., 2023), auto-immune disease, and certain neurodegenerative diseases (Frederiksen et al., 2019; Wang and Russo, 2024). These diseases also have increased prevalence in adult and aging women (Slavich and Sacher, 2019). These findings potentially provide further evidence for the hypothesis that the ability of microglia to confer vulnerability to disease shifts from being male-biased in early life, to female-biased as we age (Lynch, 2022). In conclusion, the data found in this study supports utilization of a local dsHMGB1 model to provide insight into pathological stress. Moreover, we uncover a sex-specific role for microglia in mediating responses to alarmins. Due to the ubiquitous nature PRR pathways, this work has broad potential for future work and possible utility for therapeutic development.

## 4. Materials and methods

### 4.1. Mice

All procedures involving animals were reviewed and approved by the Institutional Animal Care and Use Committee of Duke University, IACUC protocol number: 206–2310. MyD88-floxed mice were purchased from Jackson Laboratories (Bar Harbor, ME; Stock # 00888). Cx3Cr1-CreBT (MW126GSat) mice were generated and initially provided by L. Kus (GENSAT BAC Transgenic Project, Rockefeller University, NY). All methods for breeding and genotyping transgenic mice were conducted according to Rivera et al. (2019). Cx3Cr1-CreBT mice were crossed with MyD88-floxed mice over 3 generations until all offspring were fully MyD88-floxed (F/F) and either Cre negative (Cre 0/0: no modification to microglial MyD88) or Cre positive (Cre tg/0: removal of microglial MyD88), and then back-crossed onto a fully Jackson background. Genotyping of transgenic animals was conducted using polymerase chain reaction (PCR) on tail-snip DNA. Primer sequences used for PCR can be

found in Table 1. Wild-type (WT) C57BL/6J mice (used as stimuli for social preference experiments) were purchased from Jackson Laboratories (Bar Harbor, ME; Stock # 000664). All animals, age 13–20 weeks at the time of experimentation, were group housed in standard mouse cages under standard laboratory conditions (12-h light/dark cycle, 23 °C, 60 % humidity) with same-sex littermates with free access to food and water.

### 4.2. MyD88 KO recombination efficiency

For recombination efficiency experiments, microglia were isolated from cortex and hippocampus of MyD88-cKO, MyD88-CON, and C57BL/6 wild-type (WT) mice using CD11b bead isolation method (see below), and DNA was isolated from CD11b+ and CD11b-fractions. A primer set was designed to capture the recombined Exon 3 of the MyD88 allele (outside of loxP sites), with predicted band sizes for CD11b + fraction as follows: WT MyD88 Exon 3: ~600 bp, Floxed MyD88 allele, unrecombined (CON) = ~750 bp, Recombined MyD88 allele (cKO) = ~250 bp. Amount of DNA loaded into each PCR for each animal was as follows: Cd11b+ = 25 ng, Cd11b- = 100 ng, tail = 100 ng (Suppl. Fig. 4B). All primer sequences can be found in Table 1.

### 4.3. Surgery

Mice were anesthetized with 1.5 % isoflurane at a flow rate of 0.4 L/min and stereotaxically implanted with an intracerebral ventricular (ICV) guide cannula (26G, 2.25 mm from the pedestal; Plastics One, VA) into the left medial prefrontal cortex using the following coordinates from bregma (33): 1.5 mm anterior-posterior, -0.4 mm medial-lateral, and -2.25 mm dorsal-ventral from the skull. Following surgery, recovery was monitored daily, and mice were treated with saline and/or dextrose for post-operative care. After 10 days of recovery, the free moving mice were infused with 75 nl of aCSF(vehicle solution) or recombinant HMGB1 (dsHMGB1 certified LPS free (0.2ug/ul); HMGBio-tech) using a 26G internal cannula (Plastics One, VA) once daily for five consecutive days. If at anytime mice appeared to show impaired mobility or dropped below 93 % of their pre-operative body weight, they were euthanized and removed from the study. In total less than 5 % of mice were removed due to health concerns.

### 4.4. Estrus cycle analysis

Smears were obtained by vaginal cytology collected at the end of behavioral tests and stained using the heamatoxylin-eosin method. Three cell types (nucleated epithelial cells, cornified epithelial cells and leukocytes) were counted to define the reproductive cycle (estrus),

**Table 1**  
Primer Sequences for qPCR Experiments.

Primer	Sequence	Annealing Temperature C
TLR4	F: CAG CAG AGG AGA AAG CAT	55.8
	R: CAC CAG GAA TAA AGT CTC TG	
RAGE	F: AAC ACA GGA AGA ACT GAA	52.8
	R: GCC ATC GGG AAT CAG AAG TT	
MyD88	F: CAA GGC GAT GAA GAA GGA C	54.8
	R: CGC ATC AGT CTC ATC TTC CC	
MyD88 recombined (used for genotyping only)	F: TAATGGCAGTCCTCTCCCAG	60.0
	R: AGGACTACATTACCCAGGCG	
18S	F: GAA TAA TGG AAT AGG ACC GC	58.8
	R: CTT TCG CTC TGG TCC GTC TT	



which is defined by the prevalence of each cell type: proestrus (nucleated), estrus (cornified), metestrus (all types in same proportion) and diestrus (leukocytes) (Westwood, 2008). Images were acquired with a light microscope Leica DM 4000 B (Leica, Wetzlar, Germany) with a  $\times 10$  objective lens (Plan 10  $\times$  /0.25PH1).

4.5. Weight collections

Animals were weighed on the day of and the day preceding dosing. This weight was averaged to establish a baseline. Animals were weighed daily on dosing days and behavior days. The weight change reported for (Fig. 1C) is the difference between baseline weight and weight 24 h after dosing ends.

4.6. Behavioral tests

All behavioral tests were conducted approximately 12 h apart from one another alternating between light and dark phase, with the exception of feeding assays and the tail suspension test (TST). Dosing occurred in the morning/light cycle with the first test being run approximately 12 h after the administration of the final dose, during the dark cycle (Day 0). On Day 1, mice completed two behavioral assays, one in each stage of the light cycle. Following the completion of Day 1 testing, mice were subjected to food restriction (~16 h) in preparation for home cage Feeding Assay or Novelty Suppressed Feeding. The feeding assays were completed on Day 2 and immediately following completion of the assay mice were allowed unrestricted access to food (24 h). Once body weight reached approximately 98 % of pre-food restricted body weight, mice

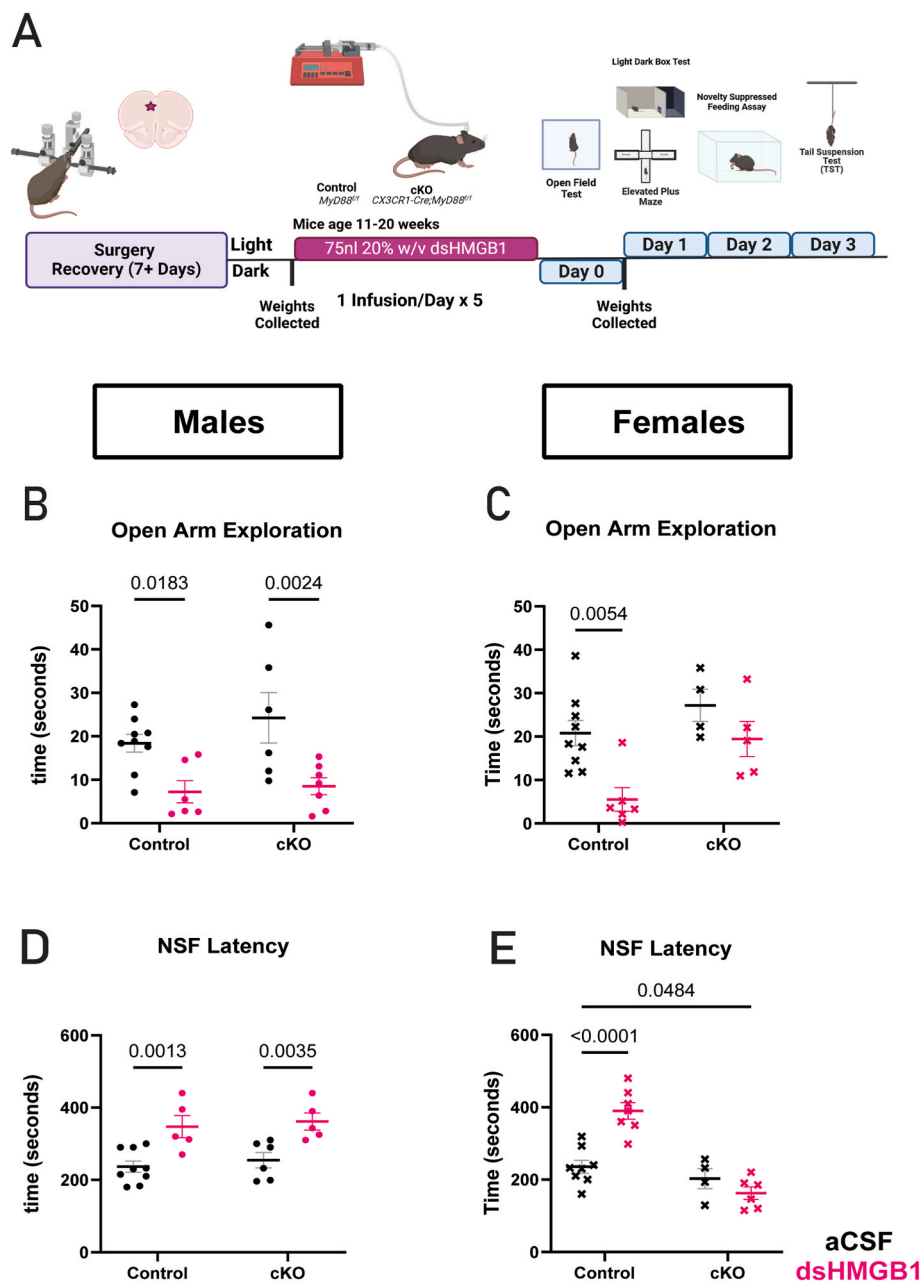


Fig. 5. Microglial MyD88 is necessary for HMGB1 response in females

(A) Schematic showing experimental outline (B) Male Time Spent in Open Arms of Elevated Plus Maze, \* $p < 0.05$ , \*\* $p < 0.01$  (C) Female Time Spent in Open Arms of Elevated Plus Maze Male (D) Male Latency to Feed in Novelty Suppressed Feeding Assay (E) Female Latency to Feed in Novelty Suppressed Feeding Assay, \* $p < 0.05$ , \*\* $p < 0.01$  N per group is 5-10, per treatment group. Statistical analyses were performed using 2-way ANOVA, Dunnett's post-hoc values displayed.

completed the tail suspension test. Mice were habituated in the testing room for at least 30 min before the test. Examiners were blinded to the groups of mice. The testing room was sound-proof and temperature controlled at 24–26 °C. After each trial, the mice were put back into their home cages and the experimental apparatus was cleaned with 75 % alcohol and Rescue cleaning solution to eliminate the odor that may affect animal behavior. Behaviors were tested in order consistent with experimental outlines provided in Figs. 1A and 5A.

#### 4.7. Open field test (OFT)

The OFT was performed in an open rectangular box with a bottom edge length of 50 cm and a height of 60 cm. The box was placed directly on the floor. After placing the mouse in the intermediate region of the box, animal behavior was recorded by a camera for 10 min. The bottom of the box was divided into the central zone (25 × 25 cm<sup>2</sup>) and the rest of the outer zone by EthovisionXT. The time spent by the animal in each region as well as the moving distance in the box were calculated.

#### 4.8. Elevated plus maze (EPM)

The apparatus used for the EPM test was a cross-shaped device consisting of an intermediate platform region (5 × 0.5 cm<sup>2</sup>) and two pairs of open arms and closed arms (25 × 5 cm<sup>2</sup>) connected to one another. The closed arms are surrounded by walls (16 cm), whereas the open arms have slight walls (0.5 cm). The entire maze was elevated to a height of 50 cm. The mouse was first placed in the intermediate region at the same position with its head toward closed arms, and its behavior in the device was then recorded by a camera for 5 min and the time spent by the animal in each arm was analyzed by EthovisionXT.

#### 4.9. Social preference assay

Social preference was measured using a two-chamber assay in which animals explored a novel object, or a novel mouse as described in (Mague et al., 2022). The assay was run in a rectangular arena (61 cm × 42.5 cm × 22 cm, L × W × H) fabricated from clear plexiglass with a clear wall separating the arena into two equal chambers with an opening in the middle allowing free access between both chambers. Plastic, circular holding cages (8.3 cm diameter and 12 cm tall) were centered in each of the two chambers and were used to hold either a novel object or sex- and age-matched C3H target mouse. The arena was evenly lit with indirect white light (~125 lux). Plastic toys and glass objects were used as novel objects with the object being between 3 and 5 cm in all directions. For the test mouse, time spent interacting with a novel object and time spent interacting with the C3H mouse were measured. Social preference ratio was calculated by normalizing the social interaction time to the object interaction time.

#### 4.10. Home Cage Feeding assay

Mice were placed in a cage with bedding material from their home cage to increase familiarity within the arena. Again, a mouse began the trial in the corner of the cage and the food pellet was placed in the center. Each trial was limited to 3 min and at the end of that time or after the mouse began its first feeding bout, the mouse was removed, and the trial completed. The latency to feed was recorded as the trial occurred and confirmed via video hand scoring.

#### 4.11. Novelty Suppressed Feeding

Following the completion of EPM, mice were food-deprived 18 h prior to the test, with free access to water. On the day of testing, mice were moved to the dimly lit testing room 1 h before the test. Mice were placed into one corner of a clear plexiglass open field apparatus (17 in. × 17 in. × 12 in.) with an opaque white acrylic floor covered with a thin

layer of home cage bedding material. The room was maintained with red light conditions. A food pellet was placed in the center of the open field and mice were placed in one corner. Latencies to approach and to begin eating were recorded with a limit of 8 min. As soon as the mouse was observed to eat, or the 8-min time limit was reached, the mouse was removed from the open field. And placed in the home cage and observed until it began to eat in the home cage.

#### 4.12. Light Dark Box test (LDB) test

The apparatus for LDB test was a rectangular box comprising two connected chambers: a light open chamber with white walls (~100 Lux, 15 × 20 × 25 cm<sup>3</sup>) and a dark covered chamber with black walls (~5 Lux, 30 × 20 × 25 cm<sup>3</sup>). The apparatus was placed on a table two feet off the ground. For every trial, the mouse was placed at the same position in the dark box. Animal behavior in the apparatus was then recorded for 8 min by a digital camera and the time the animal spent in each box was analyzed by EthovisionXT.

#### 4.13. Tail suspension test

For TST, mice were suspended from the side of a behavioral arena with white background for video tracking. At the beginning of the test, the mouse was fixed to the side of the arena with tape 1.5 cm wide and approximately 15 cm long. Mice were taped at the distal end of the tail and suspended 15 cm from the base surface. The camera was then turned on to record the animal behavior for 6 min. Immobility was defined by mobility (>2.8 %) and velocity parameters (>3 cm/s) set in EthovisionXT.

#### 4.14. Immunohistochemistry

Mice were perfused intracardially with ice-cold saline followed by phosphate-buffered 4 % paraformaldehyde (pH 7.4) after anesthetized with CO<sub>2</sub>. The brain was removed and post-fixed overnight in the same fixative and dehydrated in 30 % sucrose for 48 h at 4 °C. Coronal brain sections were cut at 30 μm by a cryostat (NX50, Thermo, USA). For immunohistochemical staining, the sections containing the mPFC and surrounding tissue containing the infralimbic and cingulate cortex, conventionally implicated in anxiety, were incubated in 0.1 % Triton X-100 for 15 min and in 5 % normal goat serum for 2 h firstly, and then were incubated with guinea pig, chicken, and rabbit anti-mouse primary antibodies against TMEM119 (1:500, Synaptic Systems, 400 004)/Iba1 (1:1000, Synaptic Systems, 234 009)/CD68 (1:500, Abcam, 125 212) overnight at 4 °C, then with anti-chicken IgG-Alexa Fluor 568 (1:1000, Invitrogen, USA), anti-rabbit IgG-Alexa Fluor 647 (1:1000, Invitrogen, USA), anti-guinea pig IgG-Alexa Fluor 488 (1:1000, Invitrogen, USA) for 2 h at room temperature (RT). After repeated washing, the sections were then covered with glass coverslips and fluorescent images were captured by a confocal microscope (Olympus FV3000 inverted confocal) utilizing a 60× objective. The analysis of fluorescence intensity and cell counting were performed by Image J software (NIH, USA). Microglia reconstructions and individual cell analysis were performed utilizing IMARIS 10.0 software. Structural analysis included the total length and the 3D arrangement of microglial branching using the Sholl analysis (number of intersections with concentric circles positioned at radial intervals of 1 μm). For each animal (3–6 per group), 6–10 microglia from mPFC were analyzed and microglia from the same animal were averaged. Observers were blinded to the experimental condition of each subject.

#### 4.15. Microglia isolation

Microglia were isolated from rodent brains using a protocol adapted from Bordt et al. (2020). Brains were dissected to grossly extract the frontal cortex as judged by the boundaries of the cannula implant. Then

sections were enzymatically digested using a dissociation cocktail containing papain or trypsin at 37 °C for 20–30 min. The tissue was then mechanically dissociated through trituration to obtain a single-cell suspension. The suspension was subjected to a density gradient centrifugation using Percoll to separate microglia from other brain cell populations. Both the microglia-enriched fraction and non-microglia enriched fraction were collected, washed, and resuspended in appropriate media for subsequent RNA isolation for the qPCR experiments.

#### 4.16. RNA extraction

Samples were homogenized in Trizol® (Thermo-fisher scientific, NY) and then vortexed for 10 min at 2000 rpm. After 15 min resting at room temperature (RT), chloroform was added (1:5 with Trizol) and samples were vortexed for 2 min at 2000 rpm. Samples were next allowed to sit at RT for 3 min and then centrifuged (15 min at 11 800 rpm; 4 °C). This resulted in a gradient from which the top, clear, aqueous phase was separated and placed into a fresh tube. Isopropanol was then added to the new tube to precipitate RNA (1:1 with aqueous phase) and samples were again vortexed, allowed to set at RT for 10 min, and then centrifuged (15 min at 11 800 rpm; 4 °C). Pellets obtained after this step were rinsed twice in ice-cold 75 % Ethanol and then resuspended in 8 µl of nuclease-free water. RNA was frozen at –80 °C until cDNA synthesis and qPCR. A NanoDrop Spectrophotometer (Thermo Scientific, Wilmington, DE) was used to determine RNA quantity and purity. RNA was considered pure enough for further use based on 260/280 (RNA:protein; range: 1.8–2.0) and 260/230 (RNA: Ethanol; range 1.6–2.0) ratios.

#### 4.17. qPCR

cDNA was synthesized using the QuantiTect Reverse Transcription Kit (Quiagen, Hilden, Germany). Briefly, 200 ng of RNA/12 µl of nuclease-free water was pre-treated with gDNase at 42 °C for 2 min to remove genomic DNA contamination. Next, master mix containing both primer-mix and reverse transcriptase was added to each sample and all samples were heated to 42 °C for 30 min and then 95 °C for 3 min (to inactivate the reaction) in the thermocycler. Quantitative real-time PCR (qPCR) was conducted using QuantiTect SYBR Green PCR Kit (Quiagen, Catalog #:204057, Hilden, Germany). To examine HMGB1-dependent signaling that is mediated by the MyD88-dependent pathways, we selected 3 genes within the signaling cascade of HMGB1 including putative receptors RAGE, TLR4, as well as MyD88 (Magna and Pisetsky, 2014). qPCR primers were designed in the lab and ordered from Integrated DNA technologies (Coralville, IA).

PCR product was monitored using a Mastercycler ep *realplex* (Eppendorf, Hauppauge, NY). Male and female samples were run on separate plates, and thus, cannot be directly compared. 18S was used as a house-keeping gene and relative gene expression was calculated using the  $2^{-\Delta\Delta CT}$  method, relative to 18S and the lowest sample on the plate (Williamson et al., 2011; Livak and Schmittgen, 2001).

#### 4.18. Statistical analysis

All data are expressed as the mean ± SEM. The required sample sizes were estimated based on our experience and Power analysis was used to justify the sample size. Statistical analysis was conducted by GraphPad Prism10.2 (GraphPad Software, USA). The Shapiro–Wilk test was used to assess whether the data followed a normal distribution. If the data was normally distributed, two-tailed Welch's *t*-test was used for comparison between two groups; if not, Mann–Whitney test was used instead. For groups with a normal distribution, a two-way ANOVA was utilized to assess the significance of two factors and the interaction of those factors (ie: sex and treatment) either Bonferroni or Dunnett's post-hoc test was used. The significance level was set at  $P < 0.05$ .

#### CRedit authorship contribution statement

**Ashleigh Rawls:** Writing – review & editing, Writing – original draft, Visualization, Methodology, Investigation, Formal analysis, Conceptualization. **Julia Dziabis:** Validation, Methodology, Investigation, Formal analysis. **Dang Nguyen:** Validation, Resources, Project administration, Investigation. **Dilara Anbarci:** Validation, Methodology, Investigation. **Madeline Clark:** Validation, Investigation, Formal analysis, Data curation. **Grace Zhang:** Methodology, Investigation, Formal analysis. **Kafui Dzirasa:** Writing – review & editing, Supervision, Resources, Methodology, Funding acquisition, Data curation, Conceptualization. **Staci D. Bilbo:** Writing – review & editing, Supervision, Resources, Project administration, Methodology, Funding acquisition, Conceptualization.

#### Funding

Research reported in this publication was supported by NIH R01-ES033056 and NIH U01 AA029969 to SDB; Hope for Depression Research Foundation, and NIH Grants 1R01MH099192 and R01MH120158 to KD.

#### Declaration of competing interest

The authors declare that they have no known competing financial interests or personal relationships that could have appeared to influence the work reported in this paper.

#### Acknowledgements

We would like to acknowledge Michael Patton, Ph.D. and Lauren Green Ph.D. for training in key techniques.

#### Appendix A. Supplementary data

Supplementary data to this article can be found online at <https://doi.org/10.1016/j.ynstr.2025.100721>.

#### References

- Amer, S.A.A.M., Fouad, A.M., El-Samahy, M., et al., 2021. Mental stress, anxiety and depressive symptoms and interleukin-6 level among healthcare workers during the COVID-19 pandemic. *J Prim Care Community Health* 12, 21501327211027432. <https://doi.org/10.1177/21501327211027432>.
- Angum, F., Khan, T., Kaler, J., Siddiqui, L., Hussain, A., 2020. The prevalence of autoimmune disorders in women: a narrative review. *Cureus* 12 (5), e8094. <https://doi.org/10.7759/cureus.8094>. Published 2020 May 13.
- Anxiety disorders. World Health Organization. September 27, 2023. Accessed April 14, 2024. <https://www.who.int/news-room/fact-sheets/detail/anxiety-disorders>.
- Bandelow, B., Michaelis, S., 2015. Epidemiology of anxiety disorders in the 21st century. *Dialogues Clin. Neurosci.* 17 (3), 327–335. <https://doi.org/10.31887/DCNS.2015.17.3/bbandelow>.
- Bassett, B., Subramaniam, S., Fan, Y., et al., 2021. Minocycline alleviates depression-like symptoms by rescuing decrease in neurogenesis in dorsal hippocampus via blocking microglia activation/phagocytosis. *Brain Behav. Immun.* 91, 519–530. <https://doi.org/10.1016/j.bbi.2020.11.009>.
- Baugher, B.J., Buckhaults, K., Case, J., Sullivan, A., Huq, S.N., Sachs, B.D., 2022. Sub-chronic stress induces similar behavioral effects in male and female mice despite sex-specific molecular adaptations in the nucleus accumbens. *Behav. Brain Res.* 425, 113811. <https://doi.org/10.1016/j.bbr.2022.113811>.
- Bollinger, J.L., Bergeon Burns, C.M., Wellman, C.L., 2016. Differential effects of stress on microglial cell activation in male and female medial prefrontal cortex. *Brain Behav. Immun.* 52, 88–97. <https://doi.org/10.1016/j.bbi.2015.10.003>.
- Bordt, EA, Block, CL, Petrozziello, T, et al., 2020. Isolation of Microglia from Mouse or Human Tissue. *STAR Protoc* 1 (1), 100035. <https://doi.org/10.1016/j.xpro.2020.100035>.
- Brydges, C.R., Bhattacharyya, S., Dehkordi, S.M., et al., 2022. Metabolomic and inflammatory signatures of symptom dimensions in major depression. *Brain Behav. Immun.* 102, 42–52. <https://doi.org/10.1016/j.bbi.2022.02.003>.
- Carvalho-Netto, E.F., Myers, B., Jones, K., Solomon, M.B., Herman, J.P., 2011. Sex differences in synaptic plasticity in stress-responsive brain regions following chronic variable stress. *Physiol. Behav.* 104 (2), 242–247. <https://doi.org/10.1016/j.physbeh.2011.01.024>.

- Cathomas, F., Holt, L.M., Parise, E.M., et al., 2022. Beyond the neuron: role of non-neuronal cells in stress disorders. *Neuron* 110 (7), 1116–1138. <https://doi.org/10.1016/j.neuron.2022.01.033>.
- Chen, X., Cui, Q.Q., Hu, X.H., et al., 2023. CD200 in dentate gyrus improves depressive-like behaviors of mice through enhancing hippocampal neurogenesis via alleviation of microglia hyperactivation. *J. Neuroinflammation* 20 (1), 157. <https://doi.org/10.1186/s12974-023-02836-4>. Published 2023 Jun 30.
- Costi, S., Morris, L.S., Collins, A., et al., 2021. Peripheral immune cell reactivity and neural response to reward in patients with depression and anhedonia. *Transl. Psychiatry* 11 (1), 565. <https://doi.org/10.1038/s41398-021-01668-1>. Published 2021 Nov 5.
- Deppermann, S., Storchak, H., Fallgatter, A.J., Ehrlis, A.C., 2014. Stress-induced neuroplasticity: (mal)adaptation to adverse life events in patients with PTSD—a critical overview. *Neuroscience* 283, 166–177. <https://doi.org/10.1016/j.neuroscience.2014.08.037>.
- Desai, M.K., Brinton, R.D., 2019. Autoimmune disease in women: endocrine transition and risk across the lifespan. *Front. Endocrinol.* 10, 265. <https://doi.org/10.3389/fendo.2019.00265>. Published 2019 Apr 29.
- Du, Y., Xu, C.L., Yu, J., et al., 2022. HMGB1 in the mPFC governs comorbid anxiety in neuropathic pain. *J. Headache Pain* 23, 102. <https://doi.org/10.1186/s10194-022-01475-z>.
- Farhane-Medina, N.Z., Luque, B., Taberner, C., Castillo-Mayén, R., 2022. Factors associated with gender and sex differences in anxiety prevalence and comorbidity: a systematic review. *Sci. Prog.* 105 (4), 368504221135469. <https://doi.org/10.1177/00368504221135469>.
- Fleshner, M., Frank, M., Maier, S.F., 2017. Danger signals and inflammasomes: stress-evoked sterile inflammation in mood disorders. *Neuropsychopharmacology* 42 (1), 36–45. <https://doi.org/10.1038/npp.2016.125>.
- Fonken, L.K., Frank, M.G., Kitt, M.M., et al., 2016. The alarmin HMGB1 mediates age-induced neuroinflammatory priming. *J. Neurosci.* 36 (30), 7946–7956. <https://doi.org/10.1523/JNEUROSCI.1161-16.2016>.
- Fonken, L.K., Frank, M.G., Gaudet, A.D., et al., 2018a. Neuroinflammatory priming to stress is differentially regulated in male and female rats. *Brain Behav. Immun.* 70, 257–267. <https://doi.org/10.1016/j.bbi.2018.03.005>.
- Fonken, L.K., Frank, M.G., Gaudet, A.D., Maier, S.F., 2018b. Stress and aging act through common mechanisms to elicit neuroinflammatory priming. *Brain Behav. Immun.* 73, 133–148. <https://doi.org/10.1016/j.bbi.2018.07.012>.
- Frank, M.G., Fonken, L.K., Annis, J.L., Watkins, L.R., Maier, S.F., 2018. Stress disinhibits microglia via down-regulation of CD200r: a mechanism of neuroinflammatory priming. *Brain Behav. Immun.* 69, 62–73. <https://doi.org/10.1016/j.bbi.2017.11.001>.
- Franklin, T.C., Wohleb, E.S., Zhang, Y., Fogaça, M., Hare, B., Duman, R.S., 2018a. Persistent increase in microglial RAGE contributes to chronic stress-induced priming of depressive-like behavior. *Biol. Psychiatry* 83 (1), 50–60. <https://doi.org/10.1016/j.biopsych.2017.06.034>.
- Franklin, T.C., Xu, C., Duman, R.S., 2018b. Depression and sterile inflammation: essential role of danger associated molecular patterns. *Brain Behav. Immun.* 72, 2–13. <https://doi.org/10.1016/j.bbi.2017.10.025>.
- Frederiksen, H.R., Haukedal, H., Freude, K., 2019. Cell type specific expression of toll-like receptors in human brains and implications in alzheimer's disease. *BioMed Res. Int.* 2019, 7420189. <https://doi.org/10.1155/2019/7420189>. Published 2019 Jul 18.
- González Ibáñez, F., Halvorson, T., Sharma, K., et al., 2023. Ketogenic diet changes microglial morphology and the hippocampal lipidomic profile differently in stress susceptible versus resistant male mice upon repeated social defeat. *Brain Behav. Immun.* 114, 383–406. <https://doi.org/10.1016/j.bbi.2023.09.006>.
- Hellmann-Regen, J., Clemens, V., Grözinger, M., et al., 2022. Effect of minocycline on depressive symptoms in patients with treatment-resistant depression: a randomized clinical trial. *JAMA Netw. Open* 5 (9), e2230367. <https://doi.org/10.1001/jamanetworkopen.2022.30367>. Published 2022 Sep. 1.
- Hinwood, M., Morandini, J., Day, T.A., Walker, F.R., 2012. Evidence that microglia mediate the neurobiological effects of chronic psychological stress on the medial prefrontal cortex. *Cereb Cortex* 22 (6), 1442–1454. <https://doi.org/10.1093/cercor/bhr229>.
- Hodes, G.E., Pfau, M.L., Leboeuf, M., et al., 2014. Individual differences in the peripheral immune system promote resilience versus susceptibility to social stress. *Proc. Natl. Acad. Sci. U. S. A.* 111 (45), 16136–16141. <https://doi.org/10.1073/pnas.1415191111>.
- Hodes, G.E., Kana, V., Menard, C., Merad, M., Russo, S.J., 2015. Neuroimmune mechanisms of depression. *Nat. Neurosci.* 18 (10), 1386–1393. <https://doi.org/10.1038/nn.4113>.
- Huang, X., Wang, B., Yang, J., Lian, Y.J., Yu, H.Z., Wang, Y.X., 2023. HMGB1 in depression: an overview of microglial HMGB1 in the pathogenesis of depression. *Brain Behav Immun Health* 30, 100641. <https://doi.org/10.1016/j.bbih.2023.100641>. Published 2023 May 25.
- Kalin, N.H., 2020. Novel insights into pathological anxiety and anxiety-related disorders. *Am. J. Psychiatr.* 177 (3), 187–189. <https://doi.org/10.1176/appi.ajp.2020.20010057>.
- Kang, R., Hou, W., Zhang, Q., et al., 2014. RAGE is essential for oncogenic KRAS-mediated hypoxic signaling in pancreatic cancer. *Cell Death Dis.* 5, e1480. <https://doi.org/10.1038/cddis.2014.445>.
- Kenwood, M.M., Kalin, N.H., Barbas, H., 2022. The prefrontal cortex, pathological anxiety, and anxiety disorders [published correction appears in *Neuropsychopharmacology* 47 (5), 1141]. <https://doi.org/10.1038/s41386-021-01216-x>. *Neuropsychopharmacology.* 2022;47(1):260-275. doi:10.1038/s41386-021-01109-z.
- Kokkosis, A.G., Madeira, M.M., Hage, Z., et al., 2024. Chronic psychosocial stress triggers microglial- macrophage- induced inflammatory responses leading to neuronal dysfunction and depressive-related behavior. *Glia* 72 (1), 111–132. <https://doi.org/10.1002/glia.24464>.
- Labonté, B., Engmann, O., Purushothaman, I., et al., 2017. Sex-specific transcriptional signatures in human depression [published correction appears in *Nat Med.* 2018 Apr 10;24(4):525]. *Nat. Med.* 23 (9), 1102–1111. <https://doi.org/10.1038/nm.4386>.
- Lehmann, M.L., Weigel, T.K., Cooper, H.A., et al., 2018. Decoding microglia responses to psychosocial stress reveals blood- brain barrier breakdown that may drive stress susceptibility. *Sci. Rep.* 8, 11240. <https://doi.org/10.1038/s41598-018-28737-8>.
- Lehmann, M.L., Weigel, T.K., Poffenberger, C.N., Herkenham, M., 2019. The behavioral sequelae of social defeat require microglia and are driven by oxidative stress in mice. *J. Neurosci.* 39 (28), 5594–5605. <https://doi.org/10.1523/JNEUROSCI.0184-19.2019>.
- Lenz, K.M., Nelson, L.H., 2018. Microglia and beyond: innate immune cells as regulators of brain development and behavioral function. *Front. Immunol.* 9, 698. <https://doi.org/10.3389/fimmu.2018.00698>. Published 2018 Apr 13.
- Lian, Y.J., Gong, H., Wu, T.Y., et al., 2017. Ds-HMGB1 and fr-HMGB1 induce depressive behavior through neuroinflammation in contrast to nonoxid-HMGB1. *Brain Behav. Immun.* 59, 322–332. <https://doi.org/10.1016/j.bbi.2016.09.017>.
- Livak, K.J., Schmittgen, T.D., 2001. Analysis of relative gene expression data using real-time quantitative PCR and the 2(-Delta Delta C(T)) Method. *Methods* 25 (4), 402–408. <https://doi.org/10.1006/meth.2001.126>.
- Lopez, J., Bagot, R.C., 2021. Defining valid chronic stress models for depression with female rodents. *Bi Psychiatry* 90 (4), 226–235. <https://doi.org/10.1016/j.biopsych.2021.03.010>.
- Lynch, M.A., 2022. Exploring sex-related differences in microglia may be a game-changer in precision medicine. *Front. Aging Neurosci.* 14, 868448. <https://doi.org/10.3389/fnagi.2022.868448>. Published 2022 Mar 31.
- Magna, M., Pisetsky, D.S., 2014. The role of HMGB1 in the pathogenesis of inflammatory and autoimmune diseases. *Mol. Med.* 20 (1), 138–146. <https://doi.org/10.2119/molmed.2013.00164>. Published 2014 Mar 24.
- Mague, S.D., Talbot, A., Blount, C., et al., 2022. Brain-wide electrical dynamics encode individual appetitive social behavior. *Neuron* 110 (10), 1728–1741.e7. <https://doi.org/10.1016/j.neuron.2022.02.016>.
- McEwen, B.S., Akil, H., 2020. Revisiting the stress concept: implications for affective disorders. *J. Neurosci.* 40 (1), 12–21. <https://doi.org/10.1523/JNEUROSCI.0733-19.2019>.
- McLean, C.P., Asnaani, A., Litz, B.T., Hofmann, S.G., 2011. Gender differences in anxiety disorders: prevalence, course of illness, comorbidity and burden of illness. *J. Psychiatr. Res.* 45 (8), 1027–1035. <https://doi.org/10.1016/j.jpsychires.2011.03.006>.
- Ménard, C., Pfau, M.L., Hodes, G.E., Russo, S.J., 2017. Immune and neuroendocrine mechanisms of stress vulnerability and resilience. *Neuropsychopharmacology* 42 (1), 62–80. <https://doi.org/10.1038/npp.2016.90>.
- Mondelli, V., Vernon, A.C., Turkheimer, F., Dazzan, P., Pariante, C.M., 2017. Brain microglia in psychiatric disorders. *Lancet Psychiatry* 4 (7), 563–572. [https://doi.org/10.1016/S2215-0366\(17\)30101-3](https://doi.org/10.1016/S2215-0366(17)30101-3).
- Nie, X., Kitaoka, S., Tanaka, K., et al., 2018. The innate immune receptors TLR2/4 mediate repeated social defeat stress-induced social avoidance through prefrontal microglial activation. *Neuron* 99 (3), 464–479.e7. <https://doi.org/10.1016/j.neuron.2018.06.035>.
- Nimmerjahn, A., Kirchhoff, F., Helmchen, F., 2005. Resting microglial cells are highly dynamic surveillants of brain parenchyma in vivo. *Science* 308 (5726), 1314–1318. <https://doi.org/10.1126/science.1110647>.
- Park, S.C., Kim, Y.K., 2020. Anxiety disorders in the DSM-5: changes, controversies, and future directions. *Adv. Exp. Med. Biol.* 1191, 187–196. [https://doi.org/10.1007/978-981-32-9705-0\\_12](https://doi.org/10.1007/978-981-32-9705-0_12).
- Pluma-Pluma, A., García, G., Murbartán, J., 2024. Chronic restraint stress and social transfer of stress produce tactile allodynia mediated by the HMGB1/TNFR1 pathway in female and male rats. *Physiol. Behav.* 274, 114418. <https://doi.org/10.1016/j.physbeh.2023.114418>.
- Rainville, J.R., Hodes, G.E., 2019. Inflaming sex differences in mood disorders. *Neuropsychopharmacology* 44 (1), 184–199. <https://doi.org/10.1038/s41386-018-0124-7>.
- Rivera, P.D., Hanamsagar, R., Kan, M.J., et al., 2019. Removal of microglial-specific MyD88 signaling alters dentate gyrus doublecortin and enhances opioid addiction-like behaviors. *Brain Behav. Immun.* 76, 104–115. <https://doi.org/10.1016/j.bbi.2018.11.010>.
- Saxena, K., Chakraborty, P., Chattarji, S., 2020. The same stress has divergent effects on social versus asocial manifestations of anxiety-like behavior over time. *Stress* 24 (4), 474–480. <https://doi.org/10.1080/10253890.2020.1855421>.
- Shimo, Y., Cathomas, F., Lin, H.Y., et al., 2023. Social stress induces autoimmune responses against the brain. *Proc. Natl. Acad. Sci. U. S. A.* 120 (49), e2305778120. <https://doi.org/10.1073/pnas.2305778120>.
- Slavich, G.M., Sacher, J., 2019. Stress, sex hormones, inflammation, and major depressive disorder: extending Social Signal Transduction Theory of Depression to account for sex differences in mood disorders. *Psychopharmacology (Berl)* 236 (10), 3063–3079. <https://doi.org/10.1007/s00213-019-05326-9>.
- Smith, C.J., Kingsbury, M.A., Dziabis, J.E., et al., 2020. Neonatal immune challenge induces female-specific changes in social behavior and somatostatin cell number. *Brain Behav. Immun.* 90, 332–345. <https://doi.org/10.1016/j.bbi.2020.08.013>.
- Sparvero, L.J., Asafu-Adjei, D., Kang, R., et al., 2009. RAGE (Receptor for Advanced Glycation Endproducts), RAGE ligands, and their role in cancer and inflammation. *J. Transl. Med.* 7, 17. <https://doi.org/10.1186/1479-5876-7-17>. Published 2009 Mar 17.

- Spiteri, A.G., Terry, R.L., Wishart, C.L., et al., 2021. High-parameter cytometry unmasks microglial cell spatio-temporal response kinetics in severe neuroinflammatory disease. *J Neuroinflammation* 18 (1), 166. Published 2021 Jul 26. doi:10.1186/s12974-021-02214-y.
- Tynan, R.J., Naicker, S., Hinwood, M., et al., 2010. Chronic stress alters the density and morphology of microglia in a subset of stress-responsive brain regions. *Brain Behav. Immun.* 24 (7), 1058–1068. <https://doi.org/10.1016/j.bbi.2010.02.001>.
- Wang, J., Russo, S.J., 2024. Neurobiology of social stress and age-related neurodegeneration. *Neurosci. Biobehav. Rev.* 156, 105482. <https://doi.org/10.1016/j.neubiorev.2023.105482>.
- Wang, B., Lian, Y.J., Su, W.J., et al., 2018. HMGB1 mediates depressive behavior induced by chronic stress through activating the kynurenine pathway. *Brain Behav. Immun.* 72, 51–60. <https://doi.org/10.1016/j.bbi.2017.11.017>.
- Wang, Y., Du, F., Hawez, A., Mörgelin, M., Thorlacius, H., 2019. Neutrophil extracellular trap-microparticle complexes trigger neutrophil recruitment via high-mobility group protein 1 (HMGB1)-toll-like receptors (TLR2)/TLR4 signalling. *Br. J. Pharmacol.* 176 (17), 3350–3363. <https://doi.org/10.1111/bph.14765>.
- Weber, M.D., McKim, D.B., Niraula, A., et al., 2019. The influence of microglial elimination and repopulation on stress sensitization induced by repeated social defeat. *Biol. Psychiatry* 85 (8), 667–678. <https://doi.org/10.1016/j.biopsych.2018.10.009>.
- Westwood, F.R., 2008. The female rat reproductive cycle: a practical histological guide to staging. *Toxicol. Pathol.* 36 (3), 375–384. <https://doi.org/10.1177/0192623308315665>.
- Williamson, LL, Sholar, PW, Mistry, RS, Smith, SH, Bilbo, SD, 2011. Microglia and memory: modulation by early-life infection. *J Neurosci* 31 (43), 15511–15521. <https://doi.org/10.1523/JNEUROSCI.3688-11.2011>.
- Won, E., Kim, Y.K., 2020. Neuroinflammation-associated alterations of the brain as potential neural biomarkers in anxiety disorders. *Int. J. Mol. Sci.* 21 (18), 6546. <https://doi.org/10.3390/ijms21186546>. Published 2020 Sep. 7.
- Woodburn, S.C., Bollinger, J.L., Wohleb, E.S., 2021. Synaptic and behavioral effects of chronic stress are linked to dynamic and sex-specific changes in microglia function and astrocyte dystrophy. *Neurobiol Stress* 14, 100312. <https://doi.org/10.1016/j.ynstr.2021.100312>. Published 2021 Mar 4.
- Xu, B., Zang, S.C., Li, S.Z., et al., 2019. HMGB1-mediated differential response on hippocampal neurotransmitter disorder and neuroinflammation in adolescent male and female mice following cold exposure. *Brain Behav. Immun.* 76, 223–235. <https://doi.org/10.1016/j.bbi.2018.11.313>.
- Xue, J., Suarez, J.S., Minaai, M., et al., 2021. HMGB1 as a therapeutic target in disease. *J. Cell. Physiol.* 236 (5), 3406–3419. <https://doi.org/10.1002/jcp.30125>.
- Yang, H., Zeng, Q., Silverman, H.A., et al., 2021. HMGB1 released from nociceptors mediates inflammation. *Proc. Natl. Acad. Sci. U. S. A.* 118 (33), e2102034118. <https://doi.org/10.1073/pnas.2102034118>.
- Yao, X.P., Ye, J., Feng, T., et al., 2023. Adaptor protein MyD88 confers the susceptibility to stress via amplifying immune danger signals. *Brain Behav. Immun.* 108, 204–220. <https://doi.org/10.1016/j.bbi.2022.12.007>.
- Yin, W., Gallagher, N.R., Sawicki, C.M., McKim, D.B., Godbout, J.P., Sheridan, J.F., 2019. Repeated social defeat in female mice induces anxiety-like behavior associated with enhanced myelopoiesis and increased monocyte accumulation in the brain. *Brain Behav. Immun.* 78, 131–142. <https://doi.org/10.1016/j.bbi.2019.01.015>.
- Zhang, S., Hu, L., Jiang, J., et al., 2020. HMGB1/RAGE axis mediates stress-induced RVLN neuroinflammation in mice via impairing mitophagy flux in microglia. *J. Neuroinflammation* 17 (1), 15. <https://doi.org/10.1186/s12974-019-1673-3>. Published 2020 Jan 10.